Math. & Comput. Sci., 6(3) 2025, 1–22

Online: ISSN 2717-2708

Mathematics and Computational Sciences

Journal Homepage: http://mcs.qut.ac.ir/mcs

Dynamics of Marburg virus in the presence of burial and cremation practices: A fractional approach

Kaushal Soni[a], Shyamsunder Kumawat[b], Arvind Kumar Sinha[a,*]

[a]Department of Mathematics, National Institute of Technology Raipur, India

[b]Department of Mathematics, SRM University Delhi-NCR Sonepat-131029, Haryana, India

Abstract

Infectious diseases have long posed a significant threat to the smooth functioning of society. To mitigate their devastating impact, we have conducted a qualitative study of the Marburg virus (MARV) transmission using a novel fractional-order model. In developing this model, we account for cultural practices, specifically burial and cremation, which are crucial in shaping the spread of the virus. The model incorporates the Caputo fractional derivative to capture memory effects in disease transmission dynamics. We have established the existence and uniqueness of solutions, along with identifying the Marburg virus free equilibrium point. Additionally, we have derived the basic reproduction number and analyzed the conditions for local stability, using the basic reproduction number as a threshold parameter. We also established Ulam-Hyers and generalized Ulam-Hyers stability. To guide effective control strategies, we perform a sensitivity analysis to determine the most impactful factors in transmission, particularly those related to contact with infected individuals and deceased bodies. Numerical simulations in MATLAB validate the theoretical results and demonstrate that reducing contact during burial and cremation processes can significantly reduce virus transmission. This study offers a comprehensive framework for understanding MARV dynamics and provides valuable insights for public health interventions.

Keywords: Marburg virus, Stability analysis, Caputo fractional derivative, Laplace transformation.

2020 MSC: 26A33, 37N25, 39B05, 44A10, 92D30

1. Introduction

The Marburg virus (MARV) is highly dangerous for human beings and comes under the family Filoviridae, which also encompasses the Ebola virus [1]. Marburg virus disease (MVD) is an uncommon yet extremely severe illness caused by MARV, a virus capable of causing widespread outbreaks and has been linked to numerous catastrophic events. MARV was initially discovered in 1967 in Marburg, Germany, during concurrent outbreaks [53]. These epidemics were linked to research projects utilizing imported African green monkeys from Uganda. Since then, Kenya, Uganda, and Angola have been among the African nations with intermittent MARV outbreaks [21, 13, 14]. The death rate for people

*Corresponding author

Email addresses: kaushalmath2205@gmail.com (Kaushal Soni), skumawatmath@gmail.com (Shyamsunder Kumawat), aksinha.maths@nitrr.ac.in (Arvind Kumar Sinha)

doi: 10.30511/mcs.2025.2050938.1293

Received: 17 January 2025 Accepted: 29 June 2025

who are infected with it is 90%. The virus can remain latent for three to nine days, with symptoms typically appearing five to ten days after infection. Early in the disease, people could have headaches, joint and muscular aches, and fever. Symptoms may get more severe as the condition advances and include nausea, eye redness, skin rash, chest pain, abdominal pain, cough, and noticeable weight loss. MARV is spread through direct contact with infected individuals or animals' bodily fluids, like urine, blood, feces, or respiratory secretions [9]. MARV consistently causes severe and often deadly hemorrhagic fever in both humans and nonhuman primates. This results in bleeding from the eyes and ears as well as internal bleeding. The fatality rate resulting from MARV sickness varies between twenty percent and eighty percent, depending on the intensity of the outbreak and the quality of medical attention available. MARV has had a considerable impact in Africa. Public health officials must be watchful and prepared to respond to new cases or outbreaks of MVD, as it can cause severe harm. The recent MARV outbreak in sub-Saharan Africa has impacted multiple countries, prompting the World Health Organization (WHO) to engage in a broad epidemiological study and proactively seek potential treatments and interventions [31].

The application of mathematical models is beneficial for exploring various dynamic aspects of a disease outbreak. Jan et al. [18] developed a mathematical model for typhoid fever that incorporates vaccination and carriers using the Caputo-Fabrizio fractional operator. In another study, Jan et al. [19] proposed a model for chikungunya virus infection that includes the effects of treatment and vaccination, formulated using the Atangana-Baleanu derivative in the sense of Caputo. Soni and Sinha [36] constructed a mathematical model for monkeypox, considering the impact of awareness and vaccination. Jain and Sinha [17] devevoped a mathematical model of efficacy of Wolbachia in malaria control with limited public health resources. Pinto et al. [30] developed an SIQR model for COVID-19. Gizachew et al. [41] conducted an analysis of a ten-compartment mathematical model for malaria transmission. Modi et al. [46] conducted a simulation-based study to estimate the spread of COVID-19 in India using the SEIR model. Kushwaha and Sinha [22] developed a mathematical model to study the vertical and horizontal transmission of malaria, incorporating intermittent preventive treatment during pregnancy. Similarly, Ambika and Sinha [6] proposed a mathematical model for cancer treatment that includes virotherapy and the role of the immune system.

These models have been instrumental in exploring various dynamic factors and controlling different diseases. Mathematical models are essential tools for comprehending and managing infectious diseases. The creation of epidemic compartmental models by experts in mathematics and biology globally has significantly advanced our understanding of MARV transmission. Over the past several decades, many articles on the transmission dynamics and control of MARV have been published. Ndendya et al. [26] proposed a mathematical model of the MARV with quarantine as a control strategy. Haque et al. [16] created a mathematical model of the MARV with isolation as a control strategy. Washachi et al. [52] developed a mathematical method of transmission of the MARV through human-to-human quarantine as a control strategy. All of these models of MARV transmision are based on traditional integer-order differential equations. Driessche and Watmough [51] have given a new technique NGM approach for calculating the basic reproduction number. Sensetivity analysis has been given by Leamer E.E [23] and frequently used by [34].

Fractional-order (FO) differential models are beneficial for examining real-life phenomena as they capture transmissible properties and memory effects that integer-order models lack. Bhattar et al. [33] developed a mathematical model for COVID-19 incorporating the impact of vaccination, utilizing the Caputo fractional derivative. Haq et al. [48] proposed a mathematical model for COVID-19 that accounts for the effects of hospitalization and quarantine, also employing the Caputo fractional derivative. Shrivastav et al. [38] studied the optimal control of a fractional-order SEIQR epidemic model with a non-monotonic incidence function and a quarantine class. Farman et al. [12] introduced a mathematical fractal-fractional model to control tuberculosis prevalence, focusing on sensitivity, stability, and simulation under feasible conditions. Masti et al. [44] analyzed a two-dimensional fractional-order brain tumor model using orthonormal Bernoulli polynomials and Newton's method. Masti et al. [45] presented an epidemiological transition model of the Ebola virus using a fractional-order framework. Jain et al. [42] investigated

Bergman's minimal blood glucose-insulin model using the Adomian Decomposition Method. Alzaid et al. [39] presented a numerical solution of an HIV-1 infection model within the framework of various fractional derivatives. Dubey et al. [40] analyzed the impact of COVID-19 in India through predictive mathematical modeling using the Atangana Baleanu fractional derivative. Sharma et al. [47] developed a Caputo fractional-order model for a predator prey system incorporating sickness in the prey and refuge for susceptible prey. Kumar et al. [43] provided numerical approximations for a groundwater flow problem using the fractional variational iteration method involving both singular and nonsingular kernel fractional derivatives. Yadav et al. [54] presented an analytical solution for a dual-porosity fractional model to simulate groundwater flow in a karstic aquifer.

The main reason for the effectiveness of models based on fractional order derivatives (FOD) is the inherent non-locality of fractional operators, often referred to as the memory effect.

The traditional derivative is extended by the introducing of various fractional operators in the literature. The idea of the FOD was introduced by Riemann and Liouville [32]. Caputo and Fabrizio [10] explored a novel differentiation approach using an exponential kernel. Aguilar et al. [15] developed a fractional Lienard-type model for pipeline dynamics using a fractional derivative without a singular kernel. Nisar et al. [27] modeled and analyzed the detrimental impact of smoking on society using the Constant Proportional Caputo Fabrizio fractional operator. Atangana and Baleanu (AB) created a FOD operator formulation using the Mittag-Leffler (ML) function as a non-local and non-singular kernel. A novel definition of FOD is grounded on a normal distribution kernel and associated ideas based on related theories [8]. Medjoudja et al. [25] proposed a fractional mathematical model based on Caputo's definition to simulate and analyze the dynamics of MARV spread influenced by fractional order terms, incorporating quarantine as a control strategy. Singh et al. [35] proposed a fractional compartmental model for the MARV, emphasizing the effectiveness of avoiding contact with recently recovered individuals to reduce infection rates. Addai et al. [1] proposed a fractionalized model of MARV based on the Caputo derivative and public health education as a control strategy. Soni and Sinha [37] proposed a fractional-order mathematical model for Marburg virus (MARV) transmission, incorporating the constraint of a limited number of hospital beds.

The novelty of this research lies in being the first to involve fractional-order calculus to analyze the transmission dynamics of the MARV, explicitly focusing on the role of burial and cremation practices. This creative approach provides a new perspective on how cultural traditions contribute to spreading disease. Furthermore, the use of advanced stability analysis techniques, such as Hyers-Ulam and generalized Hyers-Ulam, sets this study apart from traditional models, offering new insights into controlling and preventing viral outbreaks.

Classical integer-order models typically consider only the present state of the system and neglect the influence of past events. However, the transmission of Marburg virus is significantly affected by historical infection patterns and delays in community responses, especially in handling deceased individuals. The Caputo derivative enables the model to incorporate memory effects, providing a more accurate and realistic representation of disease progression.

We have clarified the advantages of our model by emphasizing that it is one of the first to incorporate burial and cremation practices into a fractional-order framework using the Caputo derivative. This allows the model to capture memory effects and historical influence on disease dynamics, which are critical in understanding and predicting Marburg virus transmission. Such modeling provides a more realistic reflection of how delayed and sustained interactions affect the outbreak, particularly through culturally rooted transmission pathways.

The significance of this study lies in its novel integration of real-world transmission factors (burial and cremation) with the mathematical power of fractional calculus. It contributes both theoretically by proving key properties of the model and practically by offering insight into how transmission can be controlled through improved practices. The findings can guide public health strategies in regions prone to Marburg virus outbreaks.

The subsequent sections of the study are organized as follows: after the Introduction in Section 1,

followed by Section 2, which presents the mathematical preliminaries of fractional calculus utilized in this article. Section 3 presents the development of the mathematical model. Section 4 presents qualitative analysis. In Section 5, we calculate the reproduction number and determine the Marburg-free equilibria, as well as their stability. Sensetivity analysis is presented in Section 6. In Section 7 we discuss the numerical technique the solution of the model (3.2). In Section 8 presented Result and discussion. Section 9 provides the conclusion of the study.

2. Preliminaries

Present section starts by exploring the essential mathematical tools that will be used in the subsequent sections.

Definition 2.1. [33] The usual definition of Laplace transformation (LT) of the function $Q(t)$ is given by

$$L[Q(t), s] = \bar{Q}(s) = \int_0^\infty e^{-st} Q(t)dt, R(s) > \Theta, t \geqslant 0. \tag{2.1}$$

Inverse LT of $\bar{P}(s)$ is given below

$$L^{-1}[\bar{\mathfrak{G}}(s), t] = \frac{1}{2\pi i}\int_{\delta-i\infty}^{\delta+i\infty} e^{st}\bar{\mathfrak{G}}(s)ds, \text{where } \delta \in \mathbb{R}. \tag{2.2}$$

Definition 2.2. [20] Let $\mathfrak{G} \in L^1([a, b], \mathbb{R})$ then the fractional integral of function $\mathfrak{G}$ define as

$$I^a_{a^+}\mathfrak{G}(t) = \frac{1}{\Gamma(a)}\int_0^t (t-s)^{a-1}\mathfrak{G}(s)ds, \tag{2.3}$$

where $a \in (0, 1])$.

Definition 2.3. [20]
The standard definition of Caputo fractional derivative (CFD) is defined as

$${}^c_0\mathfrak{D}^a_t\Theta(t) = \frac{1}{\Gamma(1-a)}\int_0^t \frac{\Theta'(s)}{(t-s)^a}ds,\ 0 < a < 1. \tag{2.4}$$

Definition 2.4. [20] LT of Caputo derivative is defined as :

$$L[{}^c_0\mathfrak{D}^a_t\Theta(t)] = s^aL[\Theta(t)]s - s^{a-1}\Theta(0). \tag{2.5}$$

Lemma 2.5. *[20]*
Consider the following assumptions for a given scenario.

$$\begin{cases} {}^c_0\mathfrak{D}^a_t\Theta(t) = \mathfrak{K}(t),\ t \in [0, \aleph],\ n-1 < a < n, \\ \Theta(0) = \Theta_0, \end{cases} \tag{2.6}$$

in which $\Theta(t) \in C[0, \aleph]$ *then* $\Theta(t) = \sum_{j=0}^{n-1} p_j t^j$ *for* $p_i \in \mathbb{R}$.

Definition 2.6. [33] The Mittag-Leffler (ML) functions $E_\rho(\mathfrak{Z})$ and $E_{\rho,\tau}(\mathfrak{Z})$ were introduced by Mittag-Leffler and Wiman, respectively.

$$E_\rho(\mathfrak{Z}) = \sum_{k=0}^\infty \frac{\mathfrak{Z}^k}{\Gamma(\rho k+1)}; (\mathfrak{Z}, \rho \in \mathbb{C}, \Re(\rho) > 0). \tag{2.7}$$

$$E_{\rho,\tau}(\mathfrak{Z}) = \sum_{k=0}^\infty \frac{\mathfrak{Z}^k}{\Gamma(\rho k+\tau)}; (\mathfrak{Z}, \rho, \tau \in \mathbb{C}, \Re(\rho) > 0, \Re(\tau) > 0). \tag{2.8}$$

3. Model formulation

We formulated a compartmental model to analyze the impact of burial and cremation practices on the transmission dynamics of the MARV. The model includes five compartments: Susceptible ($\widehat{\mathscr{V}}$), representing individuals at risk of infection; Exposed ($\widehat{\mathscr{W}}$), those who have been in contact with the virus but are not yet infectious; Infectious ($\widehat{\mathscr{X}}$), individuals capable of transmitting the virus; Recovered ($\widehat{\mathscr{Y}}$), individuals who have recovered and gained immunity; and Dead individual ($\widehat{\mathscr{Z}}$), representing deceased individuals whose burial or cremation practices may influence further transmission. At any given time t, the total human population is represented as $N(t) = \widehat{\mathscr{V}}(t) + \widehat{\mathscr{W}}(t) + \widehat{\mathscr{X}}(t) + \widehat{\mathscr{Y}}(t) + \widehat{\mathscr{Z}}(t)$. The parameters used in model Equation (3.1) are thoroughly described below.

$$\begin{cases} \frac{d\widehat{\mathscr{V}}}{dt} = \vartheta + \xi\widehat{\mathscr{Y}} - (\frac{k_1\theta_1\widehat{\mathscr{Z}}+\theta_2\widehat{\mathscr{X}}}{N} + \mu)\widehat{\mathscr{V}}, \\ \frac{d\widehat{\mathscr{W}}}{dt} = (\frac{k_1\theta_1\widehat{\mathscr{Z}}+\theta_2\widehat{\mathscr{X}}}{N})\widehat{\mathscr{V}} - (p+\mu)\widehat{\mathscr{W}}, \\ \frac{d\widehat{\mathscr{X}}}{dt} = p\widehat{\mathscr{W}} - (\mu+\delta+\eta)\widehat{\mathscr{X}}, \\ \frac{d\widehat{\mathscr{Y}}}{dt} = \eta\widehat{\mathscr{X}} - (\xi+\mu)\widehat{\mathscr{Y}}, \\ \frac{d\widehat{\mathscr{Z}}}{dt} = (\delta+\mu)\widehat{\mathscr{X}} - \beta\widehat{\mathscr{Z}}, \end{cases} \tag{3.1}$$

In the model (3.1) the dynamics of unburied deceased individuals, who can still transmit the Marburg virus. The term $(\delta+\mu)\widehat{\mathscr{X}}$ represents the inflow from infected individuals who die due to natural or disease-related causes, while $\beta\widehat{\mathscr{Z}}$ represents the outflow through burial.

where

- ϑ The recruitment rate.
- θ_1 The contact rate across susceptible individuals and deceased individuals.
- ξ The rate at which recovered individuals' short-term immunity wanes.
- θ_2 The contact rate between susceptible individuals and infected individuals.
- k_1 The proportion of deceased bodies not safely managed.
- μ The natural death rate.
- p The rate of exposed individuals moving to infected compartments.
- δ The death rate due to infection .
- η The recovery rate.
- β The rate of cremation and burial of bodies.

3.1. The fractional model

Fractional calculus has been shown to effectively model a wide range of biological systems due to its ability to capture memory and hereditary properties. In this study, we represent the aforementioned model of the Marburg virus (MARV) using fractional derivatives, as they provide more accurate and realistic results compared to classical integer-order models. Now, we consider the case where $0 < \alpha \leqslant 1$. For dimensional consistency an important aspect emphasized by Diethelm [11] must be taken to ensure that all terms involving fractional derivatives maintain consistent physical units. Thus, the proposed fractional-order model for MARV is given by:

$$\begin{cases} {}_0^c\mathfrak{D}_t^\alpha\widehat{\mathscr{V}}(t) = \vartheta^\alpha + \xi^\alpha\widehat{\mathscr{Y}} - (\frac{k_1^\alpha\theta_1^\alpha\widehat{\mathscr{Z}}+\theta_2^\alpha\widehat{\mathscr{X}}}{N} + \mu^\alpha)\widehat{\mathscr{V}}, \\ {}_0^c\mathfrak{D}_t^\alpha\widehat{\mathscr{W}}(t) = (\frac{k_1^\alpha\theta_1^\alpha\widehat{\mathscr{Z}}+\theta_2^\alpha\widehat{\mathscr{X}}}{N})\widehat{\mathscr{V}} - (p^\alpha+\mu^\alpha)\widehat{\mathscr{W}}, \\ {}_0^c\mathfrak{D}_t^\alpha\widehat{\mathscr{X}}(t) = p^\alpha\widehat{\mathscr{W}} - (\mu^\alpha+\delta^\alpha+\eta^\alpha)\widehat{\mathscr{X}}, \\ {}_0^c\mathfrak{D}_t^\alpha\widehat{\mathscr{Y}}(t) = \eta^\alpha\widehat{\mathscr{X}} - (\xi^\alpha+\mu^\alpha)\widehat{\mathscr{Y}}, \\ {}_0^c\mathfrak{D}_t^\alpha\widehat{\mathscr{Z}}(t) = (\delta^\alpha+\mu^\alpha)\widehat{\mathscr{X}} - \beta^\alpha\widehat{\mathscr{Z}}. \end{cases} \tag{3.2}$$

4. Qualitative analysis

Present section thoroughly examines the proposed model (3.2), focusing on solutions' existence, uniqueness, positivity, and boundedness. These factors are essential for evaluating the model's feasibility and its implications within a broader theoretical framework.

4.1. Solution's non-negativity and bounded

Theorem 4.1. *Consider that the initial solution of our model is* $\widehat{\mathscr{V}}(0), \widehat{\mathscr{W}}(0), \widehat{\mathscr{X}}(0), \widehat{\mathscr{Y}}(0), \widehat{\mathscr{Z}}(0) \geqslant 0$ *then solution set* $\left\{\widehat{\mathscr{V}}(t), \widehat{\mathscr{W}}(t), \widehat{\mathscr{X}}(t), \widehat{\mathscr{Y}}(t), \widehat{\mathscr{Z}}(t)\right\}$ *of the system (3.2) stays non-negative* $\forall t \geqslant 0$.

Proof. The first equation of the system (3.2)

$$
\begin{aligned}
&{}_0^c\mathfrak{D}_t^a \widehat{\mathscr{V}}(t) = \vartheta^a + \xi^a \widehat{\mathscr{Y}} - (\widehat{\mathbb{L}} + \mu^a)\widehat{\mathscr{V}},\\
&{}_0^c\mathfrak{D}_t^a \widehat{\mathscr{V}}(t) \geqslant -\mu^a \widehat{\mathscr{V}},
\end{aligned}
$$

taking LT, then we get

$$
\begin{aligned}
s^a L\left[\widehat{\mathscr{V}}(t)\right] - s^{a-1}\widehat{\mathscr{V}}(0) &\geqslant -\mu^a L\left[\widehat{\mathscr{V}}(t)\right],\\
L\left[\widehat{\mathscr{V}}(t)\right] &\geqslant \frac{s^{a-1}}{s^a + \mu^a}\widehat{\mathscr{V}}(0),
\end{aligned}
$$

taking inverse Laplace transform

$$
\widehat{\mathscr{V}}(t) \geqslant E_{a,a}(-\mu^a t^a)\big]\widehat{\mathscr{V}}(0) \geqslant 0.
$$

Similarly $\widehat{\mathscr{W}}(t) \geqslant 0, \widehat{\mathscr{X}}(t) \geqslant 0, \widehat{\mathscr{Y}}(t) \geqslant 0, \widehat{\mathscr{Z}}(t) \geqslant 0$. □

Theorem 4.2. *The solution to model (3.2) that remains uniformly bounded.*

Proof. The total population of human $\widehat{N}_1 = \widehat{N} + \widehat{\mathscr{Z}}$ the system equation can be expressed as follows:

$$
{}_0^c\mathfrak{D}_t^a \widehat{N}(t) = \vartheta^a - \mu^a \widehat{N}(t) - \delta^a \widehat{\mathscr{X}}(t),
$$

$$
{}_0^c\mathfrak{D}_t^a \widehat{N}(t) \leqslant \vartheta^a - \mu^a \widehat{N}(t).
$$

Solving the above, we get

$$
\widehat{N}(t) \leqslant E_{a,1}(-\mu^a t^a)\widehat{N}(0) + \frac{\vartheta^a}{\mu^a}(1 - E_{a,1}(-\mu^a t^a)).
$$

Utilizing the asymptotic properties of the Mittag-Leffler function [24], we derive

$$
\widehat{N}(t) \leqslant \frac{\vartheta^a}{\mu^a} \cong \mathbb{A}. \tag{4.1}
$$

From 5^{th} equation of system (3.2)

$$
{}_0^c\mathfrak{D}_t^a \widehat{\mathscr{Z}}(t) \leqslant (\delta^a + \mu^a)\mathbb{B} - \beta^a \widehat{\mathscr{Z}}(t).
$$

Solving the above, we get

$$
\widehat{\mathscr{Z}}(t) \leqslant E_{a,1}(-\beta^a t^a)N(0) + \frac{(\delta^a + \mu^a)}{\beta^a}\mathbb{B}(1 - E_{a,1}(-\beta^a t^a)),
$$

then

$$
\widehat{\mathscr{Z}}(t) \leqslant \frac{\delta^a + \mu^a}{\beta^a}\mathbb{B} \cong \mathbb{W}. \tag{4.2}
$$

Hence from Equation (4.1) and (4.2) solution of model (3.2) is bounded. □

4.2. Existence and uniqueness

Present section, we explore the qualitative aspects of the proposed fractional system (3.2) for MARV. To do so, we will begin by introducing

$$\begin{cases} \widehat{\wp}_1(t,\widehat{\mathscr{V}},\widehat{\mathscr{W}},\widehat{\mathscr{X}},\widehat{\mathscr{Y}},\widehat{\mathscr{Z}}) = \vartheta^{\alpha} + \xi^{\alpha}\widehat{\mathscr{Y}} - (\frac{k_1^{\alpha}\theta_1^{\alpha}\widehat{\mathscr{Z}}+\theta_2^{\alpha}\widehat{\mathscr{X}}}{N} + \mu^{\alpha})\widehat{\mathscr{V}}, \\ \widehat{\wp}_2(t,\widehat{\mathscr{V}},\widehat{\mathscr{W}},\widehat{\mathscr{X}},\widehat{\mathscr{Y}},\widehat{\mathscr{Z}}) = (\frac{k_1^{\alpha}\theta_1^{\alpha}\widehat{\mathscr{Z}}+\theta_2^{\alpha}\widehat{\mathscr{X}}}{N})\widehat{\mathscr{V}} - (p^{\alpha} + \mu^{\alpha})\widehat{\mathscr{W}}, \\ \widehat{\wp}_3(t,\widehat{\mathscr{V}},\widehat{\mathscr{W}},\widehat{\mathscr{X}},\widehat{\mathscr{Y}},\widehat{\mathscr{Z}}) = p^{\alpha}\widehat{\mathscr{W}} - (\mu^{\alpha} + \delta^{\alpha} + \eta^{\alpha})\widehat{\mathscr{X}}, \\ \widehat{\wp}_4(t,\widehat{\mathscr{V}},\widehat{\mathscr{W}},\widehat{\mathscr{X}},\widehat{\mathscr{Y}},\widehat{\mathscr{Z}}) = \eta^{\alpha}\widehat{\mathscr{X}} - (\xi^{\alpha} + \mu^{\alpha})\widehat{\mathscr{Y}}, \\ \widehat{\wp}_5(t,\widehat{\mathscr{V}},\widehat{\mathscr{W}},\widehat{\mathscr{X}},\widehat{\mathscr{Y}},\widehat{\mathscr{Z}}) = (\delta^{\alpha} + \mu^{\alpha})\widehat{\mathscr{X}} - \beta^{\alpha}\widehat{\mathscr{Z}}. \end{cases} \tag{4.3}$$

which can be expressed as

$$\begin{cases} {}_0^{c}\mathfrak{D}_t^{\alpha}\widehat{\wp}(t) = \Delta(t,\widehat{\wp}(t)), t \in [0,\eth], \\ \widehat{\wp}(0) = \widehat{\wp}_0 \; 0 < \alpha \leqslant 1, \end{cases} \tag{4.4}$$

where $\widehat{\wp}(t) = (\widehat{\mathscr{V}}(t), \widehat{\mathscr{W}}(t), \widehat{\mathscr{X}}(t), \widehat{\mathscr{Y}}(t), \widehat{\mathscr{Z}}(t))^{T}$ and $\widehat{\wp}_0 = (\widehat{\mathscr{V}_0}, \widehat{\mathscr{W}_0}, \widehat{\mathscr{X}_0}, \widehat{\mathscr{Y}_0}, \widehat{\mathscr{Z}_0})^{T}$,

$$\Delta(t,\widehat{\wp}(t)) = \begin{cases} \widehat{\wp}_1(t,\widehat{\mathscr{V}},\widehat{\mathscr{W}},\widehat{\mathscr{X}},\widehat{\mathscr{Y}},\widehat{\mathscr{Z}}), \\ \widehat{\wp}_2(t,\widehat{\mathscr{V}},\widehat{\mathscr{W}},\widehat{\mathscr{X}},\widehat{\mathscr{Y}},\widehat{\mathscr{Z}}), \\ \widehat{\wp}_3(t,\widehat{\mathscr{V}},\widehat{\mathscr{W}},\widehat{\mathscr{X}},\widehat{\mathscr{Y}},\widehat{\mathscr{Z}}), \\ \widehat{\wp}_4(t,\widehat{\mathscr{V}},\widehat{\mathscr{W}},\widehat{\mathscr{X}},\widehat{\mathscr{Y}},\widehat{\mathscr{Z}}), \\ \widehat{\wp}_5(t,\widehat{\mathscr{V}},\widehat{\mathscr{W}},\widehat{\mathscr{X}},\widehat{\mathscr{Y}},\widehat{\mathscr{Z}}). \end{cases} \tag{4.5}$$

Let $\mathbb{K} = C([0,\eth],\mathbb{R})$ represent the Banach space consisting of all continuous functions from the interval $[0,\eth]$ to $\mathbb{R}$, equipped with the norm defined by:

$$\|\widehat{\wp}\| = \max_{t\in[0,\eth]} |\widehat{\wp}(t)| \text{ where } |\widehat{\wp}(t)| = |\widehat{\mathscr{V}}(t)| + \widehat{\mathscr{W}}(t)| + |\widehat{\mathscr{X}}(t)| + |\widehat{\mathscr{Y}}(t)| + |\widehat{\mathscr{Z}}(t)|.$$

Here Utilized Lemma (2.5), system (4.4) can be expressed as

$$\widehat{\wp}(t) = \widehat{\wp}_0 + \frac{1}{\Gamma(\alpha)}\int_0^t (t-\Theta)^{\alpha-1}\Delta(\Theta,\widehat{\wp}(\Theta))d\Theta. \tag{4.6}$$

To examine our proposed system,we will employ the Lipschitz criterion in the following manner

I For $0 \leqslant g < 1$ $\exists$ $\mathfrak{L}_\Upsilon$ and $\wp_\Upsilon$ such that

$$|\Delta(t,\widehat{\wp}(t))| \leqslant \mathfrak{L}_\Upsilon|\widehat{\wp}|^{g} + \wp_\Upsilon. \tag{4.7}$$

II For $\mathbb{K}_\Upsilon > 0$ and $\widehat{\wp}$ and $\widehat{\wp}_\sigma \in \mathbb{K}$ we have

$$|\Delta(t,\widehat{\wp}(t)) - \Delta(t,\widehat{\wp}_\sigma(t))| \leqslant \mathbb{K}_\Upsilon|\widehat{\wp} - \widehat{\wp}_\sigma|. \tag{4.8}$$

Let us consider a map $\widehat{\aleph}$ on $\mathbb{K}$ such that

$$\widehat{\aleph}(\widehat{\wp}(t)) = \widehat{\wp}_0 + \frac{1}{\Gamma(\alpha)}\int_0^t (t-\Theta)^{\alpha-1}\Delta(\Theta,\widehat{\wp}(\Theta))d\Theta. \tag{4.9}$$

If I and II are satisfied, then there exists at least one solution to Equation (4.4). The following analysis is performed to gain deeper insight into the system.

Theorem 4.3. *If the assumptions I and II hold, then the system (3.2) has at least one solution.*

Proof. To establish the desired result, we plan to apply Schaefer's theorem. The proof will be carried out in four distinct stages, as outlined below:

A_1 : Our first objective is to confirm the continuity of $\widehat{\aleph}$. The continuity of $\Delta(t, \widehat{\wp}(t))$ will hold if we assume that $\widehat{\wp}_j$ remains continuous for $j = 1, 2, 3, 4, 5$ as we proceed, with $\widehat{\wp}, \widehat{\wp}_\sigma \in \mathbb{K}$ such that $\widehat{\wp}_\sigma \to \widehat{\wp}$ we will see that $\widehat{\aleph}(\widehat{\wp}_\sigma) \to \widehat{\aleph}(\widehat{\wp})$ In addition, take

$$\begin{aligned}
\|\widehat{\aleph}(\widehat{\wp}_\sigma) - \widehat{\aleph}(\widehat{\wp})\| &= \max_{t\in[0,\eth]} \left| \frac{1}{\Gamma(a)} \int_0^t (t-\Theta)^{a-1} \Delta(\Theta, \widehat{\wp}(\Theta)) d\Theta - \frac{1}{\Gamma(a)} \int_0^t (t-\Theta)^{a-1} \Delta(\Theta, \widehat{\wp}_\sigma(\Theta)) d\Theta \right|, \\
&\leqslant \max_{t\in[0,\eth]} \int_0^t \left| \frac{(t-\Theta)^{a-1}}{\Gamma(a)} \Big(\Delta(\Theta, \widehat{\wp}(\Theta)) - \Delta(\Theta, \widehat{\wp}_\sigma(\Theta)) \Big) \right| d\Theta, \\
&\leqslant \max_{t\in[0,\eth]} \int_0^t \left| \frac{(t-\Theta)^{a-1}}{\Gamma(a)} \right| \left| \Big(\Delta(\Theta, \widehat{\wp}(\Theta)) - \Delta(\Theta, \widehat{\wp}_\sigma(\Theta)) \Big) \right| d\Theta, \\
&\leqslant \frac{\eth^a}{\Gamma(a+1)} \mathbb{K}_\Upsilon \|\widehat{\wp} - \widehat{\wp}_\sigma\| \to 0 \quad \text{as} \quad \widehat{\wp}_\sigma \to \widehat{\wp}. \qquad (4.10)
\end{aligned}$$

Since δ^a s continuous, we obtain $\widehat{\aleph}(\widehat{\wp}_\sigma) \to \widehat{\aleph}(\widehat{\wp})$ which ensures the continuity of $\widehat{\aleph}$.

A_2 : The next step involves confirming the boundedness of the set $\widehat{\aleph}$. For every $\widehat{\wp} \in \mathbb{K}$, the operator $\widehat{\aleph}$ meets the following criteria:

$$\begin{aligned}
\|\widehat{\aleph}(\widehat{\wp})\| &= \max_{t\in[0,\eth]} \left| \widehat{\wp}_0 + \frac{1}{\Gamma(a)} \int_0^t (t-\Theta)^{a-1} \Delta(\Theta, \widehat{\wp}(\Theta)) d\Theta \right|, \\
&\leqslant |\widehat{\wp}_0| + \max_{t\in[0,\eth]} \left| \frac{1}{\Gamma(a)} \int_0^t (t-\Theta)^{a-1} \Delta(\Theta, \widehat{\wp}(\Theta)) d\Theta \right| \\
&\leqslant |\widehat{\wp}_0| + \frac{\eth^a}{\Gamma(a+1)} \Big[\mathfrak{L}_\Upsilon \|\widehat{\wp}\|^g + \wp_\Upsilon \Big]. \qquad (4.11)
\end{aligned}$$

Let $\mathfrak{A}$ is a bounded subset of $\mathbb{K}$, we aim to show that $\widehat{\aleph}(\mathfrak{A})$ is also bounded. Since $\mathfrak{A}$ is bounded, let $\widehat{\wp} \in \mathfrak{A}$ this implies the existence of some $\hbar$, such that:

$$\|\widehat{\wp}\| \leqslant \hbar, \quad \forall\ \widehat{\wp} \in \mathfrak{A}. \qquad (4.12)$$

thus, for any $\widehat{\wp} \in \mathfrak{A}$ we have the following:

$$\|\widehat{\aleph}(\widehat{\wp})\| \leqslant |\widehat{\wp}_0| + \frac{\eth^a}{\Gamma(a+1)} \Big[\mathfrak{L}_\Upsilon \|\widehat{\wp}\|^g + \wp_\Upsilon \Big] \leqslant |\widehat{\wp}_0| + \frac{\eth^a}{\Gamma(a+1)} \Big[\mathfrak{L}_\Upsilon \hbar^g + \wp_\Upsilon \Big]. \qquad (4.13)$$

Therefore, the boundedness of $\widehat{\aleph}(\mathfrak{A})$ is proved.

A_3 : To establish equi-continuity, consider $\S_1, \S_2 \in [0, \eth]$ where $\S_1 \geqslant \S_2$. Then, we have:

$$\begin{aligned}
\|\widehat{\aleph}(\widehat{\wp})(\S_1) - \widehat{\aleph}(\widehat{\wp})(\S_2)\| &= \max_{t\in[0,\eth]} \left| \frac{1}{\Gamma(a)} \int_0^{\S_1} (\S_1 - \Theta)^{a-1} \Delta(\Theta, \widehat{\wp}(\Theta)) d\Theta \right. \\
&\quad \left. - \frac{1}{\Gamma(a)} \int_0^{\S_2} (\S_2 - \Theta)^{a-1} \Delta(\Theta, \widehat{\wp}(\Theta)) d\Theta \right| \\
&\leqslant \frac{\mathfrak{L}_\Upsilon \|\widehat{\wp}\|^g + \wp_\Upsilon}{\Gamma(a+1)} [\S_1^a - \S_2^a]. \qquad (4.14)
\end{aligned}$$

As $\S_1$ approaches $\S_2$, the expression tends to zero. By the Arzela-Ascoli theorem, this implies that $\widehat{\aleph}(\mathfrak{A})$ is compact.

A_4 : Consider $\widehat{\Omega}$ such that

$$\widehat{\Omega} = \left\{ \widehat{\varphi} \in \mathbb{K} \ni \widehat{\varphi} = \upsilon \widehat{\aleph}(\widehat{\varphi}), \upsilon \in (0,1) \right\}.$$

To show that the set $\widehat{\Omega}$ is bounded, assume $\widehat{\varphi} \in \widehat{\Omega}$ and then verify that the following condition holds for $\forall t \in [0, \eth]$.

$$\|\widehat{\varphi}\| = \upsilon \|\widehat{\aleph}(\widehat{\varphi})\| \leqslant \upsilon \left(|\widehat{\varphi}_0| + \frac{\eth^{\alpha}}{\Gamma(\alpha+1)} \left[\mathfrak{L}_{\Upsilon} \|\widehat{\varphi}\|^{g} + \wp_{\Upsilon} \right] \right). \tag{4.15}$$

This indicates that the set $\widehat{\Omega}$ is bounded. By applying Schaefer's theorem, it can be concluded that the operator $\widehat{\aleph}(\widehat{\varphi})$ has a fixed point. This shows that there is at least one solution to the proposed model (3.2) for MVD. □

Remark 4.4. If condition I is fulfilled for $g = 1$ then Theorem (4.3) can be established for $\frac{\eth^{\alpha}}{\Gamma(\alpha+1)} \mathfrak{L}_{\Upsilon} < 1$.

Theorem 4.5. *There exists a unique solution of the system(3.2) exists if* $\frac{\eth^{\alpha}\, \mathbb{K}_{\Upsilon}}{\Gamma(\alpha+1)} < 1$ *holds true.*

Proof. We utilize Banach contraction theorem to achieve the desired result, assuming $\widehat{\varphi},\ \bar{\widehat{\varphi}} \in \mathbb{K}$ as:

$$\begin{aligned}
\|\widehat{\aleph}(\widehat{\varphi}) - \widehat{\aleph}(\bar{\widehat{\varphi}})\| &= \max_{t\in[0,\eth]} \left| \frac{1}{\Gamma(\alpha)} \int_0^t (t-\Theta)^{\alpha-1} \Delta(\Theta, \widehat{\varphi}(\Theta)) d\Theta - \frac{1}{\Gamma(\alpha)} \int_0^t (t-\Theta)^{\alpha-1} \Delta(\Theta, \bar{\widehat{\varphi}}(\Theta)) d\Theta \right|, \\
&= \max_{t\in[0,\eth]} \left| \frac{1}{\Gamma(\alpha)} \int_0^t (t-\Theta)^{\alpha-1} \Big(\Delta(\Theta, \widehat{\varphi}(\Theta)) - \Delta(\Theta, \bar{\widehat{\varphi}}(\Theta)) \Big) d\Theta \right|, \\
&\leqslant \max_{t\in[0,\eth]} \frac{1}{\Gamma(\alpha)} \int_0^t \left| (t-\Theta)^{\alpha-1} \Big(\Delta(\Theta, \widehat{\varphi}(\Theta)) - \Delta(\Theta, \bar{\widehat{\varphi}}(\Theta)) \Big) \right| d\Theta, \\
&\leqslant \frac{\eth^{\alpha}\, \mathbb{K}_{\Upsilon}}{\Gamma(\alpha+1)} \|\widehat{\varphi} - \bar{\widehat{\varphi}}\|.
\end{aligned} \tag{4.16}$$

Hence, it is evident that $\widehat{\aleph}$ has a unique fixed point, demonstrating that the proposed model (3.2) has a unique solution. □

4.3. Stablity analysis

Present section, we establish the stability of the proposed model (3.2) within the framework of Ulam-Hyers and generalized Ulam-Hyers stability. The concept of Ulam stability was first introduced by Ulam in [49, 50]. This type of stability has been widely studied in various works on classical fractional derivatives, as seen in [7, 5]. Since stability is essential for obtaining approximate solutions, we apply nonlinear functional analysis to explore the Ulam-Hyers and generalized stability of the proposed model (3.2). To proceed, we introduce the following necessary definitions. $\phi > 0$, and consider the inequality given below.

$$\left\| {}_0^{c}\mathfrak{D}_t^{\alpha} \widehat{\varphi}(t) - \Delta(t, \widehat{\varphi}(t)) \right\| \leqslant \varepsilon, \quad t \in [0, \eth], \tag{4.17}$$

where $\varepsilon = \max(\varepsilon_j)^{T},\ j = 1,2,3,4,5.$

Definition 4.6. The suggested problem (3.2) is considered Ulam-Hyers stable if there exists a constant $\mathfrak{E}_k > 0 \ni$, for every $\varepsilon > 0$ and for each solution $\widehat{\varphi}_{\hbar} \in \mathbb{K}$ that meets the condition (4.17) , there is a unique solution $\widehat{\varphi} \in \mathbb{K}$ of Equation (3.2), with

$$\|\widehat{\varphi}_{\hbar}(t) - \widehat{\varphi}(t)\| \leqslant \mathfrak{E}_k \varepsilon, \quad t \in [0, \eth]. \tag{4.18}$$

Where $\mathfrak{E}_k = \max(\mathfrak{E}_{k_j})^T,\ j = 1,2,3,4,5.$

Remark 4.7. A function $\widehat{\wp}_{\hbar}(t) \in \mathbb{K}$ is said to achieve inequality (4.17) iff $\exists$ a function $\mathfrak{F} \in \mathbb{K}$ has the following feature:

(a) $\|\mathfrak{F}(t)\| \leqslant \varepsilon,\ \mathfrak{F} = \max(\mathfrak{F}_j)^T,\ t \in [0, \eth]$.
(b) ${}_0^c\mathfrak{D}_t^{\alpha}\widehat{\wp}_{\hbar}(t) = \Delta(t, \widehat{\wp}_{\hbar}(t)) + \mathfrak{F}(t),\ t \in [0, \eth]$.

Theorem 4.8. *If $\widehat{\wp}_{\hbar}(t) \in \mathbb{K}$ is assumed to satisfy inequality (4.17), then $\widehat{\wp}_{\hbar}(t)$ must also satisfy the integral inequality given by*

$$\left\| \widehat{\wp}_{\hbar}(t) - \widehat{\wp}_{\hbar_0} - \frac{1}{\Gamma(\alpha)}\int_0^t (t-\Theta)^{\alpha-1}\Delta(\Theta, \widehat{\wp}_{\hbar}(\Theta))\,d\Theta \right\| \leqslant \mathfrak{G}\varepsilon. \tag{4.19}$$

Proof. From remark (4.7)
${}_0^c\mathfrak{D}_t^{\alpha}\widehat{\wp}_{\hbar}(t) = \Delta(t, \widehat{\wp}_{\hbar}(t)) + \mathfrak{F}(t),\ t \in [0, \eth]$.
From Equation (4.6)

$$\widehat{\wp}_{\hbar}(t) = \widehat{\wp}_{\hbar_0} - \frac{1}{\Gamma(\alpha)}\int_0^t (t-\Theta)^{\alpha-1}\Delta(\Theta, \widehat{\wp}_{\hbar}(\Theta))\,d\Theta - \frac{1}{\Gamma(\alpha)}\int_0^t (t-\Theta)^{\alpha-1}\mathfrak{F}(\Theta)\,d\Theta, \tag{4.20}$$

$$\left\| \widehat{\wp}_{\hbar}(t) - \widehat{\wp}_{\hbar_0} - \frac{1}{\Gamma(\alpha)}\int_0^t (t-\Theta)^{\alpha-1}\Delta(\Theta, \widehat{\wp}_{\hbar}(\Theta))\,d\Theta \right\| \leqslant \mathfrak{G}\varepsilon,$$

where $\mathfrak{G} = \frac{\eth^{\alpha}}{\Gamma(\alpha+1)}$.
Hence, the intended results. □

Theorem 4.9. *Supose that $\delta^{\alpha} : [0, \eth] \times \mathbb{R}^5 \to \mathbb{R}$ is a continuous function $\forall\ \widehat{\wp} \in \mathbb{K}$ and assumption (I) meets with $1 - \mathbb{K}_{\gamma}\mathfrak{G} > 0$. Therefore, problem (3.2) exhibits Ulam-Hyers stability and, as a result, also demonstrates generalized Ulam-Hyers stability.*

Proof. Assume that $\widehat{\wp}_{\hbar} \in \mathbb{K}$ fulfills inequality (4.17) and $\widehat{\wp} \in \mathbb{K}$ is the unique solution of (3.2). Therefore for any $\varepsilon > 0,\ t \in [0, \eth]$ and Theorem (4.8), gives:

$$\begin{aligned}
\|\widehat{\wp}_{\hbar}(t) - \widehat{\wp}(t)\| &= \max_{t\in[0,\eth]}\left|\widehat{\wp}_{\hbar}(t) - \widehat{\wp}_0 - \frac{1}{\Gamma(\alpha)}\int_0^t (t-\Theta)^{\alpha-1}\Delta(\Theta, \widehat{\wp}(\Theta))\,d\Theta\right|, \\
&\leqslant \max_{t\in[0,\eth]}\left|\widehat{\wp}_{\hbar}(t) - \widehat{\wp}_{\hbar_0} - \frac{1}{\Gamma(\alpha)}\int_0^t (t-\Theta)^{\alpha-1}\Delta(\Theta, \widehat{\wp}_{\hbar}(\Theta))\,d\Theta\right| \\
&\quad + \max_{t\in[0,\eth]}\left|\frac{1}{\Gamma(\alpha)}\int_0^t (t-\Theta)^{\alpha-1}\big(\Delta(\Theta, \widehat{\wp}(\Theta)) - \Delta(\Theta, \widehat{\wp}_{\hbar}(\Theta))\big)\,d\Theta\right|.
\end{aligned}$$

So,

$$\|\widehat{\wp}_{\hbar}(t) - \widehat{\wp}(t)\| \leqslant \mathfrak{E}_k\varepsilon,$$

where $\mathfrak{E}_k = \dfrac{\mathfrak{G}}{\left(1 - \frac{\eth^{\alpha}}{\Gamma(\alpha+1)}\mathbb{K}_{\gamma}\right)}$.
Thus, by choosing $\psi_k(\varepsilon) = \mathfrak{E}_k\varepsilon$ such that $\psi_k(0) = 0$, it follows that the problem in Equation (3.2) is both Ulam-Hyers stable and generalized Ulam-Hyers stable. □

5. Equilibria and basic reproduction number

Present section, we calculated the basic reproduction number, $\mathcal{R}_0$, and analyzed the local asymptotic stability of the MFE point.

5.1. Marburg-free equilibrium (MFE) point

To identify the equilibrium points of the fractionalized MARV model (3.2), we proceed by

$$\begin{cases} \vartheta^{\alpha} + \xi^{\alpha}\widehat{\mathscr{Y}^0} - (\frac{k_1^{\alpha}\theta_1^{\alpha}\widehat{\mathscr{Z}^0} + \theta_2^{\alpha}\widehat{\mathscr{X}^0}}{N} + \mu^{\alpha})\widehat{\mathscr{V}^0} = 0, \\ (\frac{k_1^{\alpha}\theta_1^{\alpha}\widehat{\mathscr{Z}^0} + \theta_2^{\alpha}\widehat{\mathscr{X}^0}}{N})^0\widehat{\mathscr{V}^0} - (p^{\alpha} + \mu^{\alpha})\widehat{\mathscr{W}^0} = 0, \\ p^{\alpha}\widehat{\mathscr{W}^0} - (\mu^{\alpha} + \delta^{\alpha} + \eta^{\alpha})\widehat{\mathscr{X}^0} = 0, \\ \eta^{\alpha}\widehat{\mathscr{X}^0} - (\xi^{\alpha} + \mu^{\alpha})\widehat{\mathscr{Y}^0} = 0, \\ (\delta^{\alpha} + \mu^{\alpha})\widehat{\mathscr{X}^0} - \beta^{\alpha}\widehat{\mathscr{Z}^0} = 0. \end{cases} \tag{5.1}$$

Model (3.2) remains stable without the MARV within the studied population. This occurs when $\widehat{\mathscr{W}^0} = \widehat{\mathscr{X}^0} = 0$.

Thus, the MFE denoted by $\mathfrak{W}_0$ in the model (3.2) is obtained by setting $\widehat{\mathscr{W}^0} = \widehat{\mathscr{X}^0} = 0$ in the above system.

$$\vartheta^{\alpha} - \mu^{\alpha}\widehat{\mathscr{V}^0} = 0.$$

Therefore

$$\widehat{\mathscr{V}^0} = \frac{\vartheta^{\alpha}}{\mu^{\alpha}}.$$

The MFE can be readily obtained $\mathfrak{W}_0 = \left(\frac{\vartheta^{\alpha}}{\mu^{\alpha}}, 0, 0, 0, 0\right)$.

5.2. The basic reproduction number

The basic reproduction number, R_0, is a crucial parameter in public health decision-making as it guides interventions to control the spread of infections. By lowering the contact rate, shortening the infectious period, or increasing the immune proportion of the population, R_0 can be reduced to below 1, thereby minimizing the potential impact of an epidemic. In our study, we calculate R_0 for the system using the NGM approach. This method identifies $\mathbb{F}$ and $\mathbb{V}$ from the model's infected compartments. $\mathbb{F}$ represents the progression into the infected classes, and $\mathbb{V}$ represents the removal from these classes. Our model has two infected compartments.

$$\begin{cases} {}_0^c\mathfrak{D}_t^{\alpha}\widehat{\mathscr{W}}(t) = (\frac{k_1^{\alpha}\theta_1^{\alpha}\widehat{\mathscr{Z}} + \theta_2^{\alpha}\widehat{\mathscr{X}}}{N})\widehat{\mathscr{V}} - (p^{\alpha} + \mu^{\alpha})\widehat{\mathscr{W}}, \\ {}_0^c\mathfrak{D}_t^{\alpha}\widehat{\mathscr{X}}(t) = p^{\alpha}\widehat{\mathscr{W}} - (\mu^{\alpha} + \delta^{\alpha} + \eta^{\alpha})\widehat{\mathscr{X}}, \\ {}_0^c\mathfrak{D}_t^{\alpha}\widehat{\mathscr{Z}}(t) = (\delta^{\alpha} + \mu^{\alpha})\widehat{\mathscr{X}} - \beta^{\alpha}\widehat{\mathscr{Z}}. \end{cases} \tag{5.2}$$

Based on the above, we have the following:

$$\mathbb{F} = \begin{pmatrix} (\frac{k_1^{\alpha}\theta_1^{\alpha}\widehat{\mathscr{Z}} + \theta_2^{\alpha}\widehat{\mathscr{X}}}{N})\widehat{\mathscr{V}} \\ 0 \\ 0 \end{pmatrix} \text{ and } \mathbb{V} = \begin{pmatrix} (p^{\alpha} + \mu^{\alpha})\widehat{\mathscr{W}} \\ -p^{\alpha}\widehat{\mathscr{W}} + (\mu^{\alpha} + \delta^{\alpha} + \eta^{\alpha})\widehat{\mathscr{X}} \\ -(\delta^{\alpha} + \mu^{\alpha})\widehat{\mathscr{X}} + \beta^{\alpha}\widehat{\mathscr{Z}} \end{pmatrix}.$$

Additionally, we have

$$\mathscr{F} = \begin{pmatrix} 0 & \theta_2^{\alpha} & \theta_1^{\alpha}k_1^{\alpha} \\ 0 & 0 & 0 \\ 0 & 0 & 0 \end{pmatrix}, \mathscr{V} = \begin{pmatrix} \mu^{\alpha} + p & 0 & 0 \\ -p^{\alpha} & \mu^{\alpha} + \delta^{\alpha} + \eta^{\alpha} & 0 \\ 0 & -\delta^{\alpha} - \mu^{\alpha} & \beta^{\alpha} \end{pmatrix}.$$

Since $\mathscr{F} = \frac{\partial \mathbb{F}}{\partial x}$ and $\mathscr{V} = \frac{\partial \mathbb{V}}{\partial x}$ at the equilibrium point $\mathfrak{W}_0$ the NGM is given by $\mathscr{F}\mathscr{V}^{-1}$ The basic reproduction number R_0 is the spectral radius of this NGM. Therefore $\rho(\mathscr{F}\mathscr{V}^{-1}) = R_0$ indicating that the basic reproduction number is $R_0 = R_1 + R_2$, where
$R_1 = \frac{p^{\alpha}\theta_2^{\alpha}}{(\mu^{\alpha}+\delta^{\alpha}+\eta^{\alpha})(\mu^{\alpha}+p^{\alpha})}, R_2 = \frac{p\theta_1^{\alpha}k_1^{\alpha}(\mu^{\alpha}+\delta^{\alpha})}{\beta^{\alpha}(\mu^{\alpha}+\delta^{\alpha}+\eta^{\alpha})(\mu^{\alpha}+p^{\alpha})}$.

5.3. Local stability of MFE

Theorem 5.1. *If* $R_0 < 1$, *then MFE* $\mathfrak{W}_0$ *of the proposed MARV model (3.2) is locally asymptotically stable. Conversely, if* $R_0 \geqslant 1$*the MFE becomes unstable.*

Proof. To establish the desired result, we compute the Jacobian matrix of the proposed MARV system evaluated at the MFE

$$J_{\mathfrak{W}_0}=\begin{pmatrix} -\mu^\alpha & 0 & -\theta_2^\alpha & \xi^\alpha & -\theta_1^\alpha k_1^\alpha \\ 0 & -\mu^\alpha - p^\alpha & \theta_2^\alpha & 0 & \theta_1^\alpha k_1^\alpha \\ 0 & p^\alpha & -\mu^\alpha - \delta^\alpha - \eta^\alpha & 0 & 0 \\ 0 & 0 & \eta^\alpha & -\xi^\alpha - \mu^\alpha & 0 \\ 0 & 0 & \mu^\alpha + \delta^\alpha & 0 & -\beta^\alpha \end{pmatrix}$$

MFE is considered locally stable if all eigenvalues $\lambda_j (j = 1, 2, 3, 4, 5)$ of the Jacobian matrix $J_{\mathfrak{W}_0}$ fulfill the following condition:

$$|arg(\lambda_j)| > \alpha\frac{\pi}{2}.$$

Two eigenvalues of the Jacobian matrix $J_{\mathfrak{W}_0}$ are $\lambda_1 = -\mu^\alpha$ and $\lambda_2 = -\xi^\alpha - \mu^\alpha$ then $|arg(\lambda_j)| = \pi > \alpha\frac{\pi}{2}$, $j = 1, 2, 3$ and remaining eigen values are the roots of the cubic equation

$$\lambda^3 + \beth_1\lambda^2 + \beth_2\lambda + \beth_3 = 0, \tag{5.3}$$

where

$$\beth_1 = (\mu^\alpha + p^\alpha + \beta^\alpha + \mu^\alpha + \delta^\alpha + \eta^\alpha),$$

$$\beth_2 = (\beta^\alpha(\mu^\alpha + \delta^\alpha + \eta^\alpha + \mu^\alpha + p^\alpha) + (\mu^\alpha + p^\alpha)(\mu^\alpha + \delta^\alpha + \eta^\alpha)(1 - R_1)),$$

$$\beth_3 = \beta^\alpha(\mu^\alpha + \delta^\alpha + \eta^\alpha)(\mu^\alpha + p^\alpha)(1 - R_0).$$

As per the Routh-Hurwitz criterion, the MFE is locally asymptotically stable when $R_0 < 1$, given that $\beth_1 > 0, \beth_2 > 0, \beth_3 > 0$ and $\beth_1\beth_2 - \beth_3 > 0$ Thus, it is essential to prove that all above condition fulfill when $R_0 < 1$.

It is obviously $\beth_1 = (\mu^\alpha + p^\alpha + \beta^\alpha + \mu^\alpha + \delta^\alpha + \eta^\alpha) > 0$ and moreover, when $R_0 < 1$ then $R_1 < 1$ then $\beth_2 > 0$ and $\beth_3 > 0$ and $\beth_1\beth_2 - \beth_3 = \beta^\alpha(\mu^\alpha + p^\alpha + \beta^\alpha + \mu^\alpha + \delta^\alpha + \eta^\alpha)(\mu^\alpha + \delta^\alpha + \eta^\alpha + \mu^\alpha + p^\alpha) + (1 - R_1)(\mu^\alpha + p^\alpha)(\mu^\alpha + \delta^\alpha + \eta^\alpha)(\mu^\alpha + p^\alpha + \mu^\alpha + \delta^\alpha + \eta^\alpha) + \beta^\alpha(\mu^\alpha + \delta^\alpha + \eta^\alpha)(\mu^\alpha + p^\alpha)R_2 > 0$, then roots of the Equation (5.3) have negative real part so $|arg(\lambda_j)| > \alpha\frac{\pi}{2}$, $j = 3, 4, 5$.

Therefore, the MFE exhibits local asymptotic stability when $R_0 < 1$ becomes unstable in other circumstances. □

6. Sensitivity analysis

Sensitivity analysis is necessary to evaluate how various parameters affect the spread of disease. It aids in comprehending how the reproduction number varies with specific parameters. The approach allows for the examination of crucial parameters. Once these key parameters are identified, various strategies can be devised to achieve the best possible results

The basic reproduction number, R_0, is crucial in understanding disease dynamics. The value of R_0 is determined by several parameters, estimated through collecting or observing specific data sets.

Sensitivity index of a function $\xi^\alpha(y_1, y_2, \cdots, y_n)$ for $y_i, (i = 1, 2, \cdots, n)$ is indicated by $\coprod_{y_i}^{\xi^\alpha}$ and is defined as

$$\coprod_{y_i}^{\xi^\alpha} = \frac{\partial\xi^\alpha}{\partial y_i} \times \frac{y_i}{\xi^\alpha}, \tag{6.1}$$

$$\coprod_{k_1^a}^{R_0} = \frac{p^a\theta_1^a(\mu^a+\delta^a)}{\beta^a(\mu^a+\delta^a+\eta^a)(\mu^a+p^a)},$$

$$\coprod_{\mu^a}^{R_0} = \frac{p^a(k_1^a(-\delta^{a2}+(-2\mu^a-\eta^a)\delta^a+\eta^a p^a-\mu^{a2})\theta_1^a-\beta^a\theta_2^a(p^a+2\mu^a+\eta^a+\delta^a)}{(\mu^a+\delta^a+\eta^a)^2(\mu^a+p^a)^2\beta^a},$$

$$\coprod_{\theta_1^a}^{R_0} = \frac{p^a k_1^a(\mu^a+\delta^a)}{\beta^a(\mu^a+\delta^a+\eta^a)(\mu^a+p^a)},$$

$$\coprod_{\theta_2^a}^{R_0} = \frac{p^a}{(\mu^a+\delta^a+\eta^a)(\mu^a+p^a)},$$

$$\coprod_{p^a}^{\mathcal{R}_0} = \frac{\mu^a(\theta_1^a k_1^a(\mu^a+\delta^a)+\theta_2^a\beta^a)}{\beta^a(\mu^a+\delta^a+\eta^a)(\mu^a+p^a)^2},$$

$$\coprod_{\delta^a}^{R_0} = \frac{p^a(\theta_1^a k_1^a\eta^a-\theta_2^a\beta^a)}{\beta^a(\mu^a+\delta^a+\eta^a)^2(\mu^a+p^a)},$$

$$\coprod_{\eta^a}^{R_0} = -\frac{p^a(\theta_1^a k_1^a(\mu^a+\delta^a)+\theta_2^a\beta^a)}{\beta^a(\mu^a+\delta^a+\eta^a)^2(\mu^a+p^a)},$$

$$\coprod_{\beta^a}^{R_0} = -\frac{p^a\theta_1^a k_1^a(\mu^a+\delta^a)}{\beta^{a2}(\mu^a+\delta^a+\eta^a)(\mu^a+p^a)}.$$

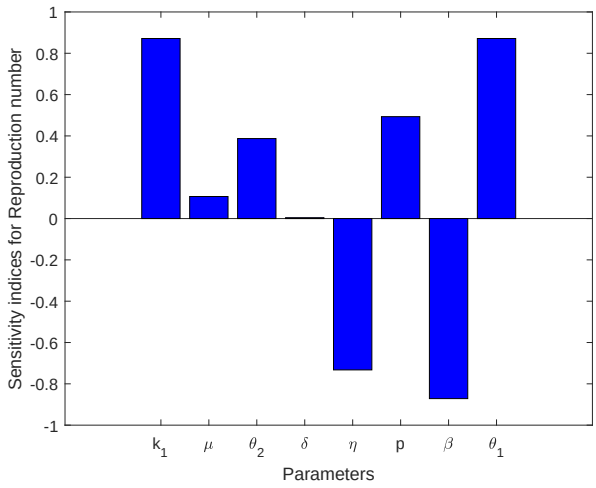

Figure 1: Sensitivity analysis of key parameters affecting R_0 at $a = 1$

Figure 1 presents the sensitivity analysis of the basic reproduction number R_0 concerning selected model parameters, evaluated at $a = 1$. The study reveals that the parameters k_1, μ, p, θ_1, and θ_2 exhibit positive sensitivity indices, indicating that an increase in any of these parameters leads to an increase in R_0. In contrast, the parameters η and β have negative sensitivity indices, implying that increases in these parameters decrease the value of R_0. This information is crucial for identifying control strategies. For instance, reducing θ_2 or increasing η (recovery rate) can effectively decrease the spread of the infection, thereby lowering R_0.

7. Methodology for the solution

Numerous compelling reasons exist for the use of numerical techniques to solve fractional ODE systems. It is well known that analytical solutions to fractional ODE issues are famously challenging and infrequently helpful due to the existence of derivatives of non-local and non-integer order in fractional calculus, as demonstrated in [4, 2]. It is frequently impossible or challenging to come up with a closed-form solution. An alternative method for approximating the solutions of fractional ODE systems is to use numerical techniques. Complex fractional ODE system modeling is made more accessible by numerical techniques. The broad range of boundary conditions, beginning conditions, and nonlinearities they provide make it easier to conduct in-depth analyses of various physical processes and systems. The analytical approaches do not work in some situations, which is where numerical methods come in. They give quick and accurate results on issues related to fractional ODEs using the tools and the algorithm. These techniques allow researchers to simulate and examine systems governed by fractional ODEs and comprehend their functionality. Because of the existence of non-local or non-integer order spatial derivatives, fractional ODE systems are normally prone to numerical instability. Fortunately, this was possible thanks to a number of sophisticated techniques that promote stabilization, inaccuracy, and implicit schemes.

In this regard, numerical procedures enable researchers to test their hypotheses under more realistic conditions because, in practice, direct experimental data are frequently unobtainable or too difficult to acquire because of the intricacy of the systems in question. Working on such systems using the numerical perspective helps back up the content validity of the models hypothesized. In addition, numerical methods can be effectively employed for the system with fractional ODEs optimization. Due to numerical search strategies, scientists are able not only to find optimal solutions, but also to investigate the parameter regions which would be impossible to probe by conventional methods.

So overall, numerical methods do come in handy when it comes to solving fractions of ODE's system especially when there is a shortage of these present.

We conducted numerical simulations of our model equations using the Generalized Euler method (GEM), which showed how different fractional orders and crucial factors alter the model's dynamics. In the context of Odibat and Momani [28], we examine the following problem. This is a generalization of Euler's typical approach.

$$ {}_0^c\mathfrak{D}_t^{\mathfrak{a}}\Theta(t) = \mathfrak{Y}(t,\Theta)\ t \in [0,T], 0 < \mathfrak{a} \leqslant 1. \tag{7.1} $$

The solution to the problem (7.1) can be located within the interval $[0,\mathfrak{W}]$ by splitting it into $\mathfrak{U}$ subintervals $[t_{\mathfrak{U}}, t_{\mathfrak{U}+1}]$ of equivalent width $h = \frac{\mathfrak{W}}{\mathfrak{U}}$ This can be achieved by using the nodes $t_{\mathfrak{U}} = \mathfrak{U}h$ for $\mathfrak{U} = 1,2,3,\ldots\mathfrak{W}$ Expand Θ about $t = t_0 = 0$ and employ the generalized Taylor's formula [29]. Consider that on $[0,\mathfrak{W}]$ Θ, ${}_0^c\mathfrak{D}_t^{\mathfrak{a}}\Theta(t)$, ${}_0^c\mathfrak{D}_t^{2\mathfrak{a}}\Theta(t)$ are continuous functions. As a result, for each t, there exists a corresponding value $\aleph$ implying that

$$ \Theta(t) = \Theta(t_0) + ({}_0^c\mathfrak{D}_t^{\mathfrak{a}}\Theta(t))(t_0)\frac{t^{\mathfrak{a}}}{\Gamma(\mathfrak{a}+1)} + ({}_0^c\mathfrak{D}_t^{2\mathfrak{a}}\Theta(t))\aleph\frac{t^{2\mathfrak{a}}}{\Gamma(2\mathfrak{a}+1)}. \tag{7.2} $$

When $({}_0^c\mathfrak{D}_t^{\mathfrak{a}}\Theta(t))(t_0) = \mathfrak{Y}(t_0,\Theta(t_0))$ and $h = t_1$ are replaced in Equation (7.2). The outcome is a formula for $\Theta(t_1)$:

$$ \Theta(t_1) = \Theta(t_0) + \mathfrak{Y}(t_0,\Theta(t_0))\frac{h^{\mathfrak{a}}}{\Gamma(\mathfrak{a}+1)} + ({}_0^c\mathfrak{D}_t^{2\mathfrak{a}}\Theta(t))\aleph\frac{h^{2\mathfrak{a}}}{\Gamma(2\mathfrak{a}+1)}. \tag{7.3} $$

The solution can be obtained by ignoring the second-order term (involving $h^{2\mathfrak{a}}$) when the step size h is sufficiently small

$$ \Theta(t_1) = \Theta(t_0) + \mathfrak{Y}(t_0,\Theta(t_0))\frac{h^{\mathfrak{a}}}{\Gamma(\mathfrak{a}+1)}. \tag{7.4} $$

Continue this process until a sequence of points approximates the solution $\Theta(t)$. When $t_{\mathfrak{U}+1} = t_{\mathfrak{U}} + h$ the formula for

$$\Theta(t_{\mathfrak{U}+1}) = \Theta(t_{\mathfrak{U}}) + \frac{h^{a}}{\Gamma(a+1)}\mathfrak{Y}(t_{\mathfrak{U}}, \Theta(t_{\mathfrak{U}})), \tag{7.5}$$

for $\mathfrak{U} = 1, 2, 3, \ldots \mathfrak{W}$ It is obvious that for $a = 1$. The GEM (7.5) reduces to the classical Euler's method, Thus

$$\widehat{\mathscr{V}}(t_{\mathfrak{U}+1}) = \widehat{\mathscr{V}}(t_{\mathfrak{U}}) + \frac{h^{a}}{\Gamma(a+1)}\left[\vartheta^{a} + \xi^{a}\widehat{\mathscr{Y}}(t_{\mathfrak{U}}) - \left(\frac{k_1^{a}\theta_1^{a}\widehat{\mathscr{Z}}(t_{\mathfrak{U}}) + \theta_2^{a}\widehat{\mathscr{X}}(t_{\mathfrak{U}})}{N} + \mu^{a}\right)\widehat{\mathscr{V}}(t_{\mathfrak{U}})\right],$$

$$\widehat{\mathscr{W}}(t_{\mathfrak{U}+1}) = \widehat{\mathscr{W}}(t_{\mathfrak{U}}) + \frac{h^{a}}{\Gamma(a+1)}\left[\left(\frac{k_1^{a}\theta_1^{a}\widehat{\mathscr{Z}}(t_{\mathfrak{U}}) + \theta_2^{a}\widehat{\mathscr{X}}(t_{\mathfrak{U}})}{N}\right)\widehat{\mathscr{V}}(t_{\mathfrak{U}}) - (p^{a} + \mu^{a})\widehat{\mathscr{W}}(t_{\mathfrak{U}})\right],$$

$$\widehat{\mathscr{X}}(t_{\mathfrak{U}+1}) = \widehat{\mathscr{X}}(t_{\mathfrak{U}}) + \frac{h^{a}}{\Gamma(a+1)}\left[p^{a}\widehat{\mathscr{W}}(t_{\mathfrak{U}}) - (\mu^{a} + \delta^{a} + \eta^{a})\widehat{\mathscr{X}}(t_{\mathfrak{U}})\right],$$

$$\widehat{\mathscr{Y}}(t_{\mathfrak{U}+1}) = \widehat{\mathscr{Y}}(t_{\mathfrak{U}}) + \frac{h^{a}}{\Gamma(a+1)}\left[\eta^{a}\widehat{\mathscr{X}}(t_{\mathfrak{U}}) - (\xi^{a} + \mu^{a})\widehat{\mathscr{Y}}(t_{\mathfrak{U}})\right],$$

$$\widehat{\mathscr{Z}}(t_{\mathfrak{U}+1}) = \widehat{\mathscr{Z}}(t_{\mathfrak{U}}) + \frac{h^{a}}{\Gamma(a+1)}\left[(\delta^{a} + \mu^{a})\widehat{\mathscr{X}}(t_{\mathfrak{U}}) - \beta^{a}\widehat{\mathscr{Z}}(t_{\mathfrak{U}})\right].$$

In doing so, one gets

$$\widehat{\mathscr{V}}_{\mathfrak{v}+1} = \widehat{\mathscr{V}}_{\mathfrak{v}} + \mathscr{T}\left[\vartheta^{a} + \xi^{a}\widehat{\mathscr{Y}}_{\mathfrak{v}} - \left(\frac{k_1^{a}\theta_1^{a}\widehat{\mathscr{Z}}_{\mathfrak{v}} + \theta_2^{a}\widehat{\mathscr{X}}_{\mathfrak{v}}}{N} + \mu^{a}\right)\widehat{\mathscr{V}}_{\mathfrak{v}}\right],$$

$$\widehat{\mathscr{W}}_{\mathfrak{v}+1} = \widehat{\mathscr{W}}_{\mathfrak{v}} + \mathscr{T}\left[\left(\frac{k_1^{a}\theta_1^{a}\widehat{\mathscr{Z}}_{\mathfrak{v}} + \theta_2^{a}\widehat{\mathscr{X}}_{\mathfrak{v}}}{N}\right)\widehat{\mathscr{V}}_{\mathfrak{v}} - (p^{a} + \mu^{a})\widehat{\mathscr{W}}_{\mathfrak{v}}\right],$$

$$\widehat{\mathscr{X}}_{\mathfrak{v}+1} = \widehat{\mathscr{X}}_{\mathfrak{v}} + \mathscr{T}\left[p^{a}\widehat{\mathscr{W}}_{\mathfrak{v}} - (\mu^{a} + \delta^{a} + \eta^{a})\widehat{\mathscr{X}}_{\mathfrak{v}}\right],$$

$$\widehat{\mathscr{Y}}_{\mathfrak{v}+1} = \widehat{\mathscr{Y}}_{\mathfrak{v}} + \mathscr{T}\left[\eta^{a}\widehat{\mathscr{X}}_{\mathfrak{v}} - (\xi^{a} + \mu^{a})\widehat{\mathscr{Y}}_{\mathfrak{v}}\right],$$

$$\widehat{\mathscr{Z}}_{\mathfrak{v}+1} = \widehat{\mathscr{Z}}_{\mathfrak{v}} + \mathscr{T}\left[(\delta^{a} + \mu^{a})\widehat{\mathscr{X}}_{\mathfrak{v}} - \beta^{a}\widehat{\mathscr{Z}}_{\mathfrak{v}}\right].$$

Where the step size $0 < \mathscr{T} = \frac{h^{a}}{\Gamma(a+1)} < 1$ depends on the beginning circumstances $\widehat{\mathscr{V}_0}, \widehat{\mathscr{W}_0}, \widehat{\mathscr{X}_0}, \widehat{\mathscr{Y}_0}, \widehat{\mathscr{Z}_0}$. We have $\widehat{\mathscr{V}}_{\mathfrak{v}+1} = \widehat{\mathscr{V}}_{\mathfrak{v}} = \widehat{\mathscr{V}}, \widehat{\mathscr{W}}_{\mathfrak{v}+1} = \widehat{\mathscr{W}}_{\mathfrak{v}} = \widehat{\mathscr{W}}, \widehat{\mathscr{X}}_{\mathfrak{v}+1} = \widehat{\mathscr{X}}_{\mathfrak{v}} = \widehat{\mathscr{X}}, \widehat{\mathscr{Y}}_{\mathfrak{v}+1} = \widehat{\mathscr{Y}}_{\mathfrak{v}} = \widehat{\mathscr{Y}}, \widehat{\mathscr{Z}}_{\mathfrak{v}+1} = \widehat{\mathscr{Z}}_{\mathfrak{v}} = \widehat{\mathscr{Z}}$ at a fixed point.

8. Result and discussion

Present section, we provide numerical results about different values of the fractional order a and other sufficiently important parameters to verify our theoretical results and analyze their effect on the dynamics of our model. The values of the parameters employed in this model are summarized in Table 1, including both those sourced from existing literature and those assumed based on biological reasoning. Simulations were carried out to assess the influence of various factors on the spread of MARV infection and potential mitigation strategies using MATLAB21.
Figure

Table 1: Parameters with their values for fractional order model

parameter	Value	Source
ϑ	400	Assumed
θ_1	0.952	Assumed
ξ	0.004	[16]
θ_2	0.28	[25]
k_1	[0, 1]	Assumed
μ	0.146	[3]
p	0.050	[1]
δ	0.001	[1]
η	0.4027	[16]
β	[0, 1]	Assumed

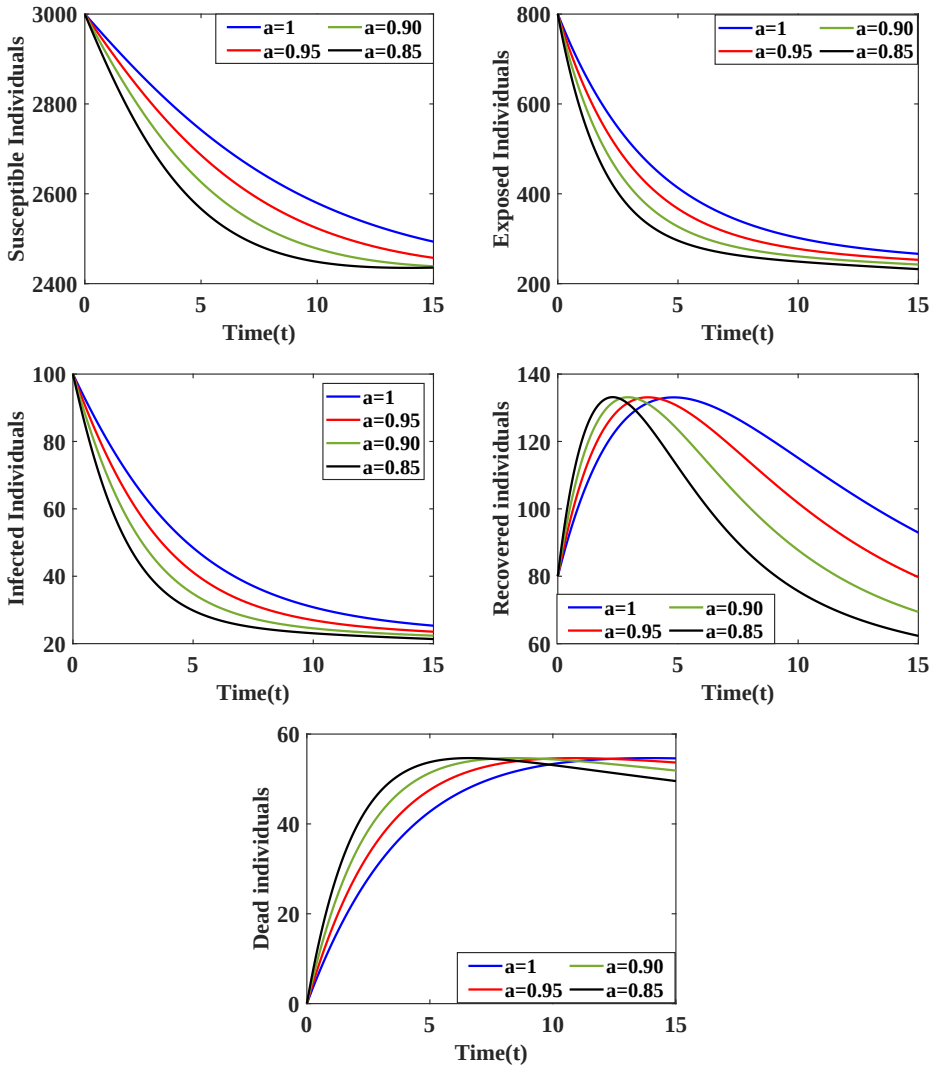

Figure 2: The dynamics of population at different fractional-order values

Figure 3 illustrates the effect of the parameter k_1, which represents the proportion of deceased bodies that are not safely managed. As shown in Figure 3(a) demonstrates that the value of k_1 increases from 0.28, 0.48, 0.78, and 0.99 the susceptible population declines. Mean while, Figures 3(b), 3(c), 3(d), and

3(e) show that the exposed, infected, recovered, and deceased populations increase, respectively. This indicates that poor management of deceased bodies leads to a heightened risk of disease transmission, reducing the number of susceptible individuals while increasing exposure and infection rates. Figure 4

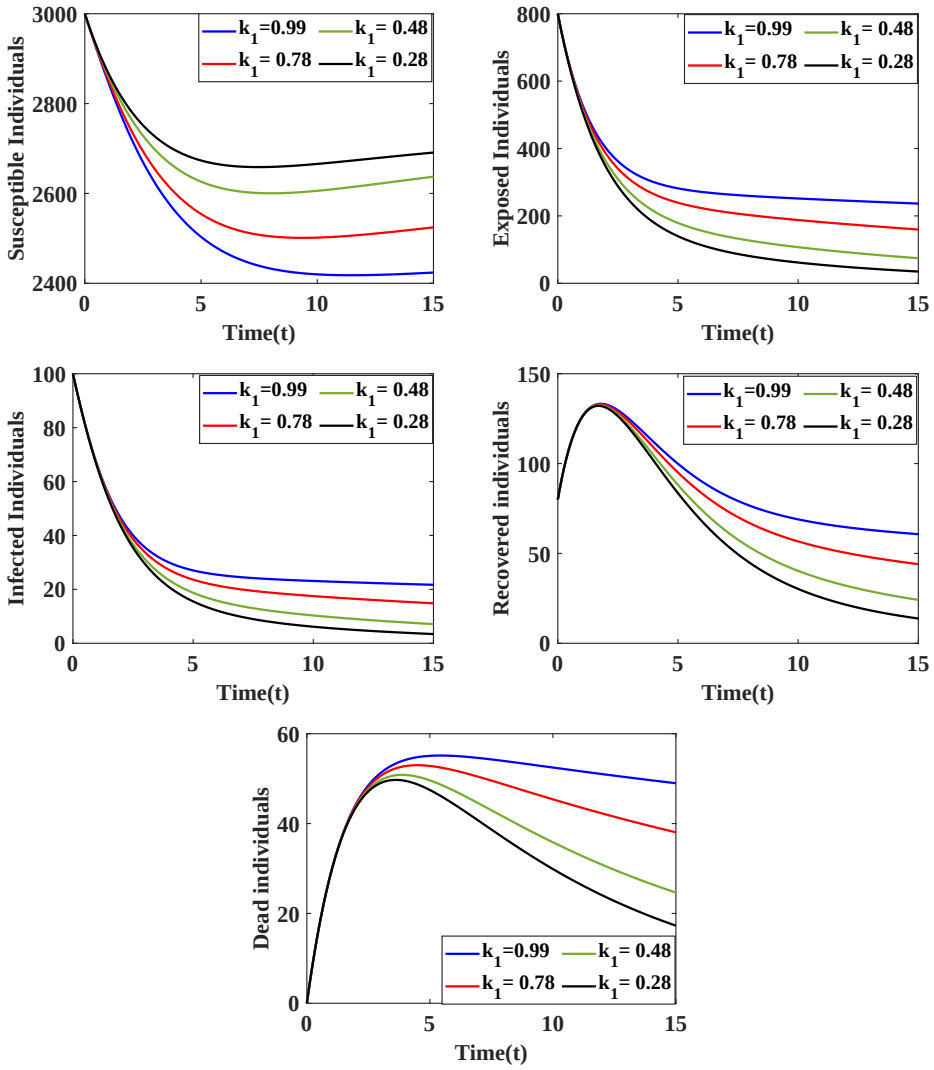

Figure 3: The dynamics of the population at different values of parameter k_1

shows the impact of the parameter θ_1 represents the effective contact rate between susceptible individuals and deceased bodies. As shown in Figure 4(a), increasing θ_1 From 0.6, 0.7,0.8, and 0.9 leads to a decline in the susceptible population. Meanwhile, Figures 4(b), 4(c), 4(d), and 4(e) illustrate corresponding increases in the exposed, infected, recovered, and deceased populations. These results indicate that a higher contact rate with improperly managed deceased bodies substantially contributes to the transmission of infection. Figure 5 illustrates the influence of the parameter θ_2, which signifies the effective rate of contact between susceptible and infected individuals. Figure 5(a) demonstrates that the value of θ_2 increase from 0.28, 0.68, 0.78, and0.98 then susceptible population decreases and Figures 5(b), 5(c), 5(d), and 5(e) reveal an increase in the exposed, infected, recovered, and deceased populations, respectively, with rising values of θ_2. This underscores the importance of minimizing contact with infected individuals to control the spread of infection.

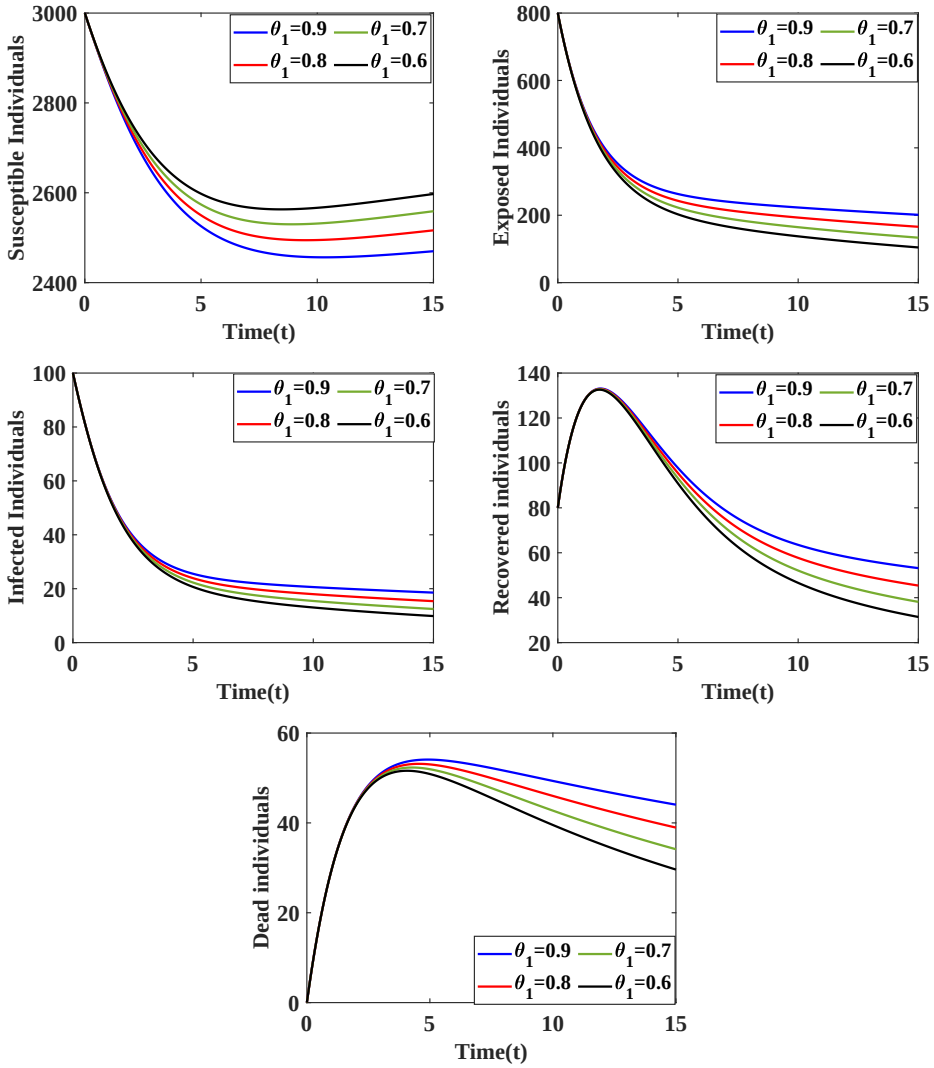

Figure 4: The dynamics of the population at different values of parameter θ_1

9. Conclusion

This study constructed a fractional-order epidemic model for the MARV, considering the impacts of memory trace and customary burial and cremation rituals while concentrating on the infection's dynamic properties. This innovative method provides new perspectives on funeral traditions' social and cultural dimensions. The model's equilibrium point has been determined, and theorems and proofs have been used to assess their asymptotic stability thoroughly. The fundamental reproduction number was determined by utilizing the NGM approach, guaranteeing biological feasibility in both the bounded and positive sections of the model.

Furthermore, an investigation was conducted on the uniqueness and presence of positive global solutions for the fractional-order MARV model. The Hyers-Ulam and Generalized Hyers-Ulam stability theories were used to develop stability findings. The model was expanded upon to get approximations for the system's solutions, and the generalized Euler technique was utilized to obtain approximations. Fractional ordinary differential equations may be effectively solved with this approach, which combines explicit and implicit approaches to produce precise and dependable numerical solutions. These sophisticated computational methods allowed for the visualization of the fractional-order derivative's memory trace, providing more understanding of the dynamics and behavior of the model. The study concluded that several model parameters were the most detrimental to the dynamic process. According to simulations,

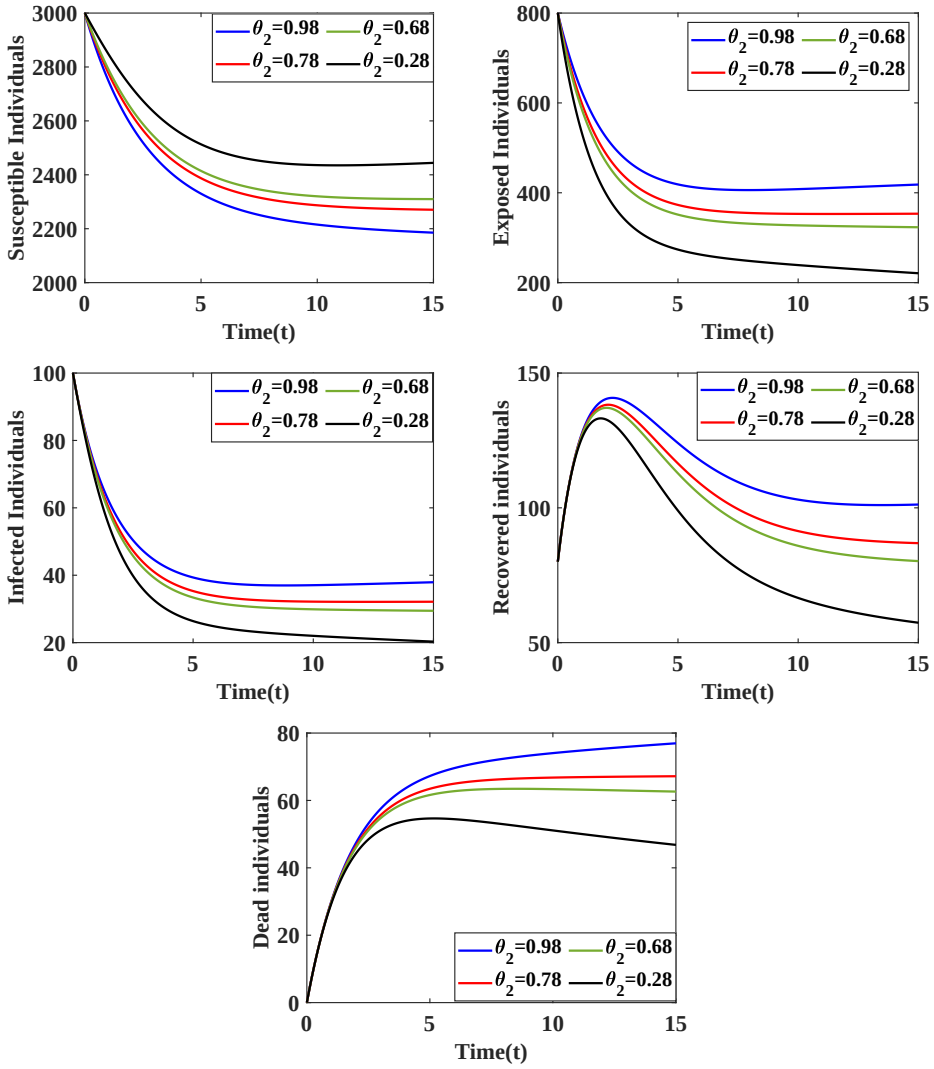

Figure 5: The dynamics of the population at different values of parameter θ_2

adhering to integrated containment strategies significantly decreased the infection rate. The article's numerical results for the fractional-order model led to the conclusion that the basic reproduction number (R_0) and the model parameters directly impact whether the illness is eliminated or becomes prevalent. The study's findings, particularly the application of fractional-order derivatives, provide a more thorough examination of the dynamic behavior of the MARV epidemic model at every step. These findings are especially relevant to policymakers and public health experts, as they take memory effects into account and provide a more realistic and complete examination of the disease's evolution than typical integer-order derivatives. The results of this study can significantly enhance the creation of treatment and disease control methods, thereby improving major epidemic response and prevention skills and providing important guidance for decision-making.

In summary, this study highlights the significance of sophisticated mathematical models for enhancing the precision and efficiency of MARV management. These models aid in the creation of more accurate control methods for MARV and related problems. By capturing the historical behavior and memory effects of illnesses that conventional integer-order models frequently miss, the addition of fractional-order derivatives enhances mathematical epidemiology. With the long-term consequences of past states on present dynamics taken into account, this technique offers a more realistic simulation of illness transmission and development. Better fitting of empirical data, enhanced parameter estimates, and improved model validation are also made possible by the flexibility of the Caputo derivative.

Furthermore, fractional-order models, with their ability to recognize different stages of infection and intricate dynamics, offer a deeper understanding of control and preventive tactics. This understanding has the potential to significantly improve disease transmission understanding, enhance outbreak forecasting accuracy, and lead to the development of more effective public health treatments. Future studies should focus on creating higher-quality fractional-order models that incorporate ecological elements including age structure, weather, and environmental impacts. These models, which could be created utilizing various fractional operators, such as Caputo-Fabrizio or Atangana-Baleanu, have the potential to significantly improve healthcare management and model accuracy, thereby increasing our knowledge of disease dynamics and forecast accuracy.

Declaration of competing interest

- None of the authors of this paper has a financial or personal relationship with other people or organizations that could inappropriately influence or bias the content of the paper.
- It is to specifically state that No Competing interests are at stake, and there is No Conflict of Interest with other people or organizations that could inappropriately influence or bias the content of the paper.

Data availability

No data was used for the research described in the article.

Acknowledgments

The authors are extremely thankful to the Department of Mathematics, National Institute of Technology Raipur (C. G.), India, for providing facilities, space, and an opportunity for the work.

References

[1] Addai, E., Adeniji, A., Ngungu, M., Tawiah, G.K., Marinda, E., Asamoah, J.K.K., Khan, M.A. (2023). A nonlinear fractional epidemic model for the marburg virus transmission with public health education. Scientific Reports, 13(1), 19292. 1, 1

[2] Ahmad, H., Khan, M.N., Ahmad, I., Omri, M., Alotaibi, M.F.(2023). A meshless method for numerical solutions of linear and nonlinear time-fractional black-scholes models. AIMS Math, 8(8):19677–19698. 7

[3] Ajelli, M. and Merler, S. (2012). Transmission potential and design of adequate control measures for marburg hemorrhagic fever. PloS one, 7(12):e50948. 1

[4] Al-Shomrani, M.M., Musa, S.S., and Yusuf, A. (2023). Unfolding the transmission dynamics of monkeypox virus: an epidemiological modelling analysis. Mathematics, 11(5):1121. 7

[5] Ali, Z., Kumam, P., Shah, K., and Zada, A. (2019). Investigation of ulam stability results of a coupled system of nonlinear implicit fractional differential equations. Mathematics, 7(4):341. 4.3

[6] Ambika and Sinha, A.K. (2025). Mathematical model of cancer treatment with virotherapy and immune system. Critical Reviews in Biomedical Engineering, 53(3). 1

[7] Aphithana, A., Ntouyas, S.K., and Tariboon, J. (2019). Existence and ulam–hyers stability for caputo conformable differential equations with four-point integral conditions. Advances in Difference Equations, 2019:1–17. 4.3

[8] Atangana, A. and Gómez-Aguilar, J.F. (2017). A new derivative with normal distribution kernel: Theory, methods and applications. Physica A: Statistical mechanics and its applications, 476:1–14. 1

[9] Bharat, T.A., Riches, J.D., Kolesnikova, L., Welsch, S., Krähling, V., Davey, N., Parsy, M.L., Becker, S., and Briggs, J.A. (2011). Cryo-electron tomography of marburg virus particles and their morphogenesis within infected cells. PLoS biology, 9(11):e1001196. 1

[10] Caputo, M. and Fabrizio, M. (2015). A new definition of fractional derivative without singular kernel. Progress in Fractional Differentiation & Applications, 1(2):73–85. 1

[11] Diethelm, K. (2013). A fractional calculus based model for the simulation of an outbreak of dengue fever. Nonlinear Dynamics, 71:613–619. 3.1

[12] Farman, M., Shehzad, A., Nisar, K.S., Hincal, E., and Akgul, A. (2024). A mathematical fractal-fractional model to control tuberculosis prevalence with sensitivity, stability, and simulation under feasible circumstances. Computers in Biology and Medicine, 178:108756. 1
[13] Feldmann, H., Slenczka, W., and Klenk, H.-D. (1996). Emerging and reemerging of filoviruses. Springer. 1
[14] Gear, J.S., Cassel, G., Gear, A., Trappler, B., Clausen, L., Meyers, A., Kew, M., Bothwell, T., Sher, R., Miller, G., et al. (1975). Outbreake of marburg virus disease in johannesburg. Br Med J, 4(5995):489–493. 1
[15] Gómez-Aguilar, J., Torres, L., Yépez-Martínez, H., Baleanu, D., Reyes, J., and Sosa, I. (2016). Fractional liénard type model of a pipeline within the fractional derivative without singular kernel. Advances in Difference Equations, 2016:1–13. 1
[16] Haque, Z., Kamrujjaman, M., Alam, M., and Biswas, M. (2024). Marburg virus and risk factor among infected population: A modeling study. Malaysian Journal of Mathematical Sciences, 18(1). 1, 1
[17] Jain, H. and Sinha, A.K. (2025). Modeling the efficacy of wolbachia in malaria control with limited public health resources. Nonlinear Analysis: Real World Applications, 84:104325. 1
[18] Jan, R., Boulaaras, S., Alnegga, M., and Abdullah, F. A. (2024). Fractional-calculus analysis of the dynamics of typhoid fever with the effect of vaccination and carriers. International Journal of Numerical Modelling: Electronic Networks, Devices and Fields, 37(2):e3184. 1
[19] Jan, R., Razak, N. N. A., Boulaaras, S., Rajagopal, K., Khan, Z., and Almalki, Y. (2023). Fractional perspective evaluation of chikungunya infection with saturated incidence functions. Alexandria Engineering Journal, 83:35–42. 1
[20] Kilbas, A. (2006). Theory and applications of fractional differential equations. 204. 2.2, 2.3, 2.4, 2.5
[21] Kuhn, J. H., Dürrwald, R., Bào, Y., Briese, T., Carbone, K., Clawson, A. N., Derisi, J. L., Garten, W., Jahrling, P. B., Kolodziejek, J., et al. (2015). Taxonomic reorganization of the family bornaviridae. Archives of virology, 160:621–632. 1
[22] Kushavaha, S. K. and Sinha, A. K. (2024). Modeling the vertical and horizontal transmission of malaria with intermittent preventive treatment in pregnancy. SeMA Journal, pages 1–27. 1
[23] Leamer, E. E. (1985). Sensitivity analyses would help. The American Economic Review, 75(3):308–313. 1
[24] Li, H.-L., Zhang, L., Hu, C., Jiang, Y.-L., and Teng, Z. (2017). Dynamical analysis of a fractional-order predator-prey model incorporating a prey refuge. Journal of Applied Mathematics and Computing, 54:435–449. 4.2
[25] Medjoudja, M., El hadi Mezabia, M., Riaz, M. B., Boudaoui, A., Ullah, S., and Awwad, F. A. (2024). A novel computational fractional modeling approach for the global dynamics and optimal control strategies in mitigating marburg infection. AIMS Mathematics, 9(5):13159–13194. 1, 1
[26] Ndendya, J. Z., Mureithik, E., Mwasunda, J. A., and Kagaruki, G. B. (2024). Mathematical modeling and analysis of marburg virus disease dynamics. SSRN. 1
[27] Nisar, K. S., Farman, M., Hincal, E., and Shehzad, A. (2023). Modelling and analysis of bad impact of smoking in society with constant proportional-caputo fabrizio operator. Chaos, Solitons & Fractals, 172:113549. 1
[28] Odibat, Z. M. and Momani, S. (2008). An algorithm for the numerical solution of differential equations of fractional order. Journal of Applied Mathematics & Informatics, 26(1):15–27. 7
[29] Odibat, Z. M. and Shawagfeh, N. T. (2007). Generalized taylors formula. Applied Mathematics and computation, 186(1):286–293. 7
[30] Pinto, C. M., Tenreiro Machado, J., and Burgos-Simón, C. (2024). Modified siqr model for the covid-19 outbreak in several countries. Mathematical Methods in the Applied Sciences, 47(5):3273–3288. 1
[31] Sah, R., Reda, A., Lashin, B. I., Abdelaal, A., Mohanty, A., Siddiq, A., and Padhi, B. K. (2022). Marburg virus and monkeypox virus: The concurrent outbreaks in ghana and the lesson learned from the marburg virus containment. J. Pure Appl. Microbiol, 16(1):3179–3184. 1
[32] Samko, S. G. (1993). Fractional integrals and derivatives. Theory and applications. 1
[33] Shyamsunder, Bhatter, S., Jangid, K., Abidemi, A., Owolabi, K. M., and Purohit, S. D. (2023). A new fractional mathematical model to study the impact of vaccination on covid-19 outbreaks. Decision Analytics Journal, 6:100156. 1, 2.1, 2.6
[34] Shyamsunder and Purohit, S. D. (2024). A novel study of the impact of vaccination on pneumonia via fractional approach. Partial Differential Equations in Applied Mathematics, 10:100698. 1
[35] Singh, J. P., Abdeljawad, T., Baleanu, D., and Kumar, S. (2023). Transmission dynamics of a novel fractional model for the marburg virus and recommended actions. The European Physical Journal Special Topics, 232(14):2645–2655. 1
[36] Soni, K. and Sinha, A. K. (2024a). Modeling and stability analysis of the transmission dynamics of monkeypox with control intervention. Partial Differential Equations in Applied Mathematics, 10:100730. 1
[37] Soni, K. and Sinha, A. K. (2024b). Modeling marburg virus control with limited hospital beds: a fractional approach. Physica Scripta, 100(1):015251. 1
[38] Srivastava, A. et al. (2024). Optimal control of a fractional order seiqr epidemic model with non-monotonic incidence and quarantine class. Computers in Biology and Medicine, page 108682. 1
[39] Alzaid, S.S. and Alkahtani, B.S.T. and Sharma, S. and Dubey, R.S. (2021). Numerical Solution of Fractional Model of HIV-1 Infection in Framework of Different Fractional Derivatives. Journal of Function Spaces, 2021(1):6642957. 1

[40] Dubey, R.S. and Mishra, M.N. and Goswami, P. (2022). Effect of Covid-19 in India-A prediction through mathematical modeling using Atangana Baleanu fractional derivative. Journal of Interdisciplinary Mathematics, 25(8):2431–2444. 1

[41] Gellow, G.T. and Munganga, J.M.W. and Jafari, H. (2023). ANALYSIS OF A TEN COMPARTMENTAL MATHEMATICAL MODEL OF MALARIA TRANSMISSION. Advanced Mathematical Models &Applications, 8(2). 1

[42] Jain, R. and Arekar, K. and Dubey, R.S. (2017). Study of Bergman's minimal blood glucose-insulin model by Adomian decomposition method. Journal of Information and Optimization Sciences, 38(1), 133–149. 1

[43] Kumar, P. and Yadav, M.P. (2024). Numerical approximations of groundwater flow problem using fractional variational iteration method with fractional derivative of singular and nonsingular kernels. International Journal of Mathematics for Industry, 16:2450008. 1

[44] Masti, I. and Sayevand, K. and Jafari, H. (2024). On analyzing two dimensional fractional order brain tumor model based on orthonormal Bernoulli polynomials and Newton's method. An International Journal of Optimization and Control: Theories & Applications (IJOCTA), 14(1):12–19. 1

[45] Masti, I. and Sayevand, K. and Jafari, H. (2024). ON EPIDEMIOLOGICAL TRANSITION MODEL OF THE EBOLA VIRUS IN FRACTIONAL SENSE. Journal of Applied Analysis and Computation, 14(3):1625–1647. 1

[46] Modi, K. and Umate, L. and Makade, K. and Dubey, R.S. and Agarwal, P. (2021). Simulation based study for estimation of COVID-19 spread in India using SEIR model. Journal of Interdisciplinary Mathematics, 24(2):245–258. 1

[47] Sharma, S. and Dubey, R.S. and Chaudhary, A. (2024). Caputo fractional model for the predator–prey relation with sickness in prey and refuge to susceptible prey. International Journal of Mathematics for Industry, 1:1–12. 1

[48] Ul Haq, I., Ali, N., Bariq, A., Akgül, A., Baleanu, D., and Bayram, M. (2024). Mathematical modelling of covid-19 outbreak using caputo fractional derivative: stability analysis. Applied Mathematics in Science and Engineering, 32(1):2326982. 1

[49] Ulam, S. M. (1960). A collection of mathematical problems. (Interscience Publishers), 8. 4.3

[50] Ulam, S. M. (2004). Problems in modern mathematics. Courier Corporation. 4.3

[51] Van den Driessche, P. and Watmough, J. (2002). Reproduction numbers and sub-threshold endemic equilibria for compartmental models of disease transmission. Mathematical biosciences, 180(1-2):29–48. 1

[52] Washachi, J.D., Amoka, J.A., Orapine, H.O., and Baidu, A.A. (2023). Mathematical modelling of transmission dynamics of marburg virus with effective quarantine approach. CaJoST, 5(3):264–272. 1

[53] WHO (2022). World marburg virus report, world health organization. 1

[54] Yadav, M.P., Agarwal, R., Purohit, S.D., Kumar, D., and Suthar, D.L. (2022). Groundwater flow in karstic aquifer: analytic solution of dual-porosity fractional model to simulate groundwater flow. Applied Mathematics in Science and Engineering, 30(1):598–608. 1